A Novel Somatostatin Mimic with Broad Somatotropin Release Inhibitory Factor Receptor Binding and Superior Therapeutic Potential

Ian Lewis,* Wilfried Bauer, Rainer Albert, Nagarajan Chandramouli, Janos Pless, Gisbert Weckbecker, and Christian Bruns

Transplantation Research Department, Novartis Pharma, CH-4002 Basel, Switzerland

Received November 12, 2002

A rational drug design approach, capitalizing on structure−activity relationships and involving transposition of functional groups from somatotropin release inhibitory factor (SRIF) into a reduced size cyclohexapeptide template, has led to the discovery of SOM230 (**25**), a novel, stable cyclohexapeptide somatostatin mimic that exhibits unique high-affinity binding to human somatostatin receptors (subtypes sst1−sst5). SOM230 has potent, long-lasting inhibitory effects on growth hormone and insulin-like growth factor-1 release and is a promising development candidate currently under evaluation in phase I clinical trials.

1. Introduction

Somatotropin release inhibitory factor (SRIF) (**1**), a tetradecapeptide discovered by Brazeau et al.,[1] has been shown to have potent inhibitory effects on various secretory processes in tissues such as pituitary, pancreas, and gastrointestinal tract. SRIF also acts as a neuromodulator in the central nervous system.[2]

The biological effects of SRIF, almost all inhibitory in nature, are elicited through a family of G-protein-coupled receptors, of which five different subtypes have been characterized, termed sst1−sst5.[3]

Cloning of five SRIF receptors has been achieved from human, rat, mouse, porcine, and bovine tissues.[4−8] The amino acid sequence of SRIF receptors range from 363 (sst5) to 418 (sst2) amino acids, and the sequence homology varies from 39% to 57% between receptor subtypes. Greater sequence homology is seen in the sequences of the transmembrane domains compared to the extracellular and intracellular loops. The highest sequence homology is evident between sst_1 and sst_4 and among sst_2, sst_3, and sst_5, and each individual receptor subtype shows high sequence homology among species (81−98% among mouse, human, and rat homologues).[9]

The effects associated with single sst subtypes have been reviewed extensively.[5,10] The functional characterization of single sst subtypes is, however, limited because of the lack of highly selective antagonists for all sst subtypes. The SRIF receptor subtype sst1 can mediate antiproliferative effects. The main receptor subtype is sst2, which mediates both antisecretory and antiproliferative action. Ligation of sst2 inhibits secretion of GH, glucagon, gastrin, and gastric acid and inhibits ion secretion in the colon. Sst2 is expressed on a number of cancers including small-cell lung and gastro-entero-pancreatic tumors and mediates tumor cell growth inhibition. Subtype sst3 was reported to mediate antiproliferative and proapoptotic effects. The role of sst4, which is expressed at high levels in the lung, is not well understood, while sst5 has been shown to mediate inhibition of GH and cell proliferation.

The five somatostatin receptor subtypes have similar high affinities for the natural SRIF ligand SRIF-14 (**1**).[4] However, potent smaller SRIF agonists have been synthesized that differ from SRIF in their affinities for the different subtypes (Figure 1).[11−15]

In the present approach, transposition of functional groups from endogenous SRIF, determined to be responsible for the unique affinity of SRIF to different somatostatin receptor subtypes, into a reduced size, stable cyclohexapeptide template has for the first time led to the identification of a somatostatin mimic that exhibits unique high-affinity binding to four of the five human somatostatin receptors (sst1−sst5).

The unique pharmacological effects mediated by SRIF-14[1] (**1**) are derived from its universal high-affinity binding to all somatostatin receptor subtypes sst1−sst5. However, SRIF-14 (**1**) has a very short in vivo half-life of less than 3 min, limiting its therapeutic utility in man.[16]

The short-chain synthetic octapeptide SMS 201-995 (octreotide, Sandostatin)[11] (**2**, Figure 1) was introduced into clinical practice in 1987 for treatment of hormone-secreting pituitary adenomas and gastroenteropancreatic (GEP) tumors. Since then, **2** has remained the mainstay of SRIF analogue therapy and provides considerably broader therapeutic application[17] because of its enhanced in vivo stability.

Compound **2**,[11] along with BIM 23014 (**3**),[12,13] the cyclooctapeptide RC160 (**4**),[14,15] and the Merck cyclohexapeptide MK-678 (**5**) and closely related analogues **6** and **7**,[18−23] displays high affinity for sst2 only, moderate affinity for sst3 and sst5, and no or low affinity for sst1 and sst4 (Table 1).

Conceptually, the combination of the unique pharmacological effects of SRIF-14 (**1**) due to its high-affinity binding to sst1−sst5 with the proven in vivo stability of short-chain synthetic mimics, such as the cyclohexapeptide **(5)** discovered by Veber and co-workers, was extremely attractive. Indeed, the challenging goal

* To whom correspondence should be addressed. Phone: +41 61 324 3762. Fax: +4161 324 7821. E-mail:ian.lewis@pharma.novartis.com.

10.1021/jm021093t CCC: $25.00
Published on Web 05/13/2003

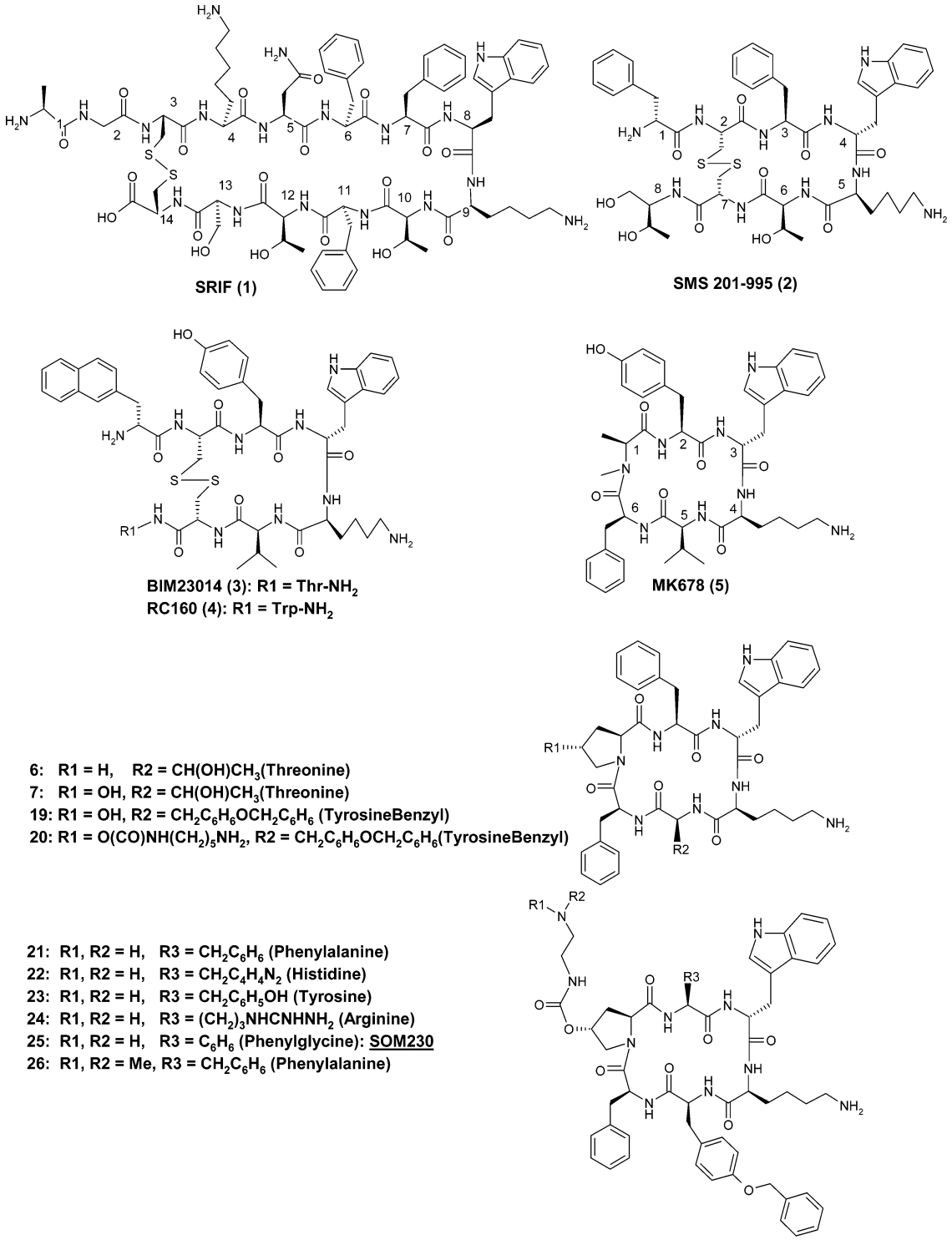

Figure 1. Structures of SRIF-14, Sandostatin, SOM230, and related analogues.

of this research was to design a smaller, stable SRIF-14 mimic that exhibits a more universal high-affinity binding to sst1−sst5 and that may consequently exhibit superior therapeutic utility in patients with GH release disorders such as acromegaly.[24] To achieve this goal, we adopted a strategy involving transposing structural groups from SRIF-14 (**1**) determined to be responsible for high-affinity binding to different somatostatin receptor subtypes into a reduced size, stable cyclohexapeptide template. In contrast to earlier investigations aimed at identifying analogues that are subtype-selective for sst2,[25,26] the long-term goal of this investigation was to determine if our strategy to achieve broad SRIF receptor binding would be rewarded in terms of superior therapeutic potential of such a reduced size, more universal somatostatin mimic.[24]

2. Results

2.1. Synthesis. SRIF analogues (**8**−**18**, Table 1), where each residue is replaced by alanine in turn (except residues 3 and 14, forming the disulfide bridge as well as residue 1, already an alanine), were synthesized on solid phase using the Fmoc/^{t}Bu strategy and the Rink amide linker.[27,28] Cleavage and deprotection

Table 1. Binding of Somatostatin Analogues to SRIF Receptor Subtypes (pK_i)

		pK_i				
		sst1	sst2	sst3	sst4	sst5
1	SRIF-14: H-Ala-Gly-{Cys-Lys-Asn-Phe-Phe-Trp-Lys-Thr-Phe-Thr-Ser-Cys}-OH	9.2	9.7	9.6	8.9	9.4
2	SMS 201-995: H-D-Phe-{Cys-Phe-D-Trp-Lys-Thr-Cys}-Thr(ol)	6.6	9.5	8.3	≤6.0	8.3
3	BIM 23014: lanreotide, H-D-(*β*)Nal-{Cys-Tyr-D-Trp-Lys-Val-Cys}-Thr-NH_2	6.3	9.3	7.2	<6.0	8.4
4	RC 160: H-D-Phe-{Cys-Tyr-D-Trp-Lys-Val-Cys}-Trp-NH_2	6.8	10.1	7.7	6.8	8.3
5	MK678: cyclo[MeAla-Tyr-D-Trp-Lys-Val-Phe]	<6.0	10.1	7.5	<6.0	7.9
6	cyclo[Pro-Phe-D-Trp-Lys-Thr-Phe]	6.2	9.2	6.9	<7.0	7.4
7	cyclo[HyPro-Phe-D-Trp-Lys-Thr-Phe]	<6.0	9.7	6.7	<6.0	<6.0
8	Ala^2-SRIF-14-NH_2: H-Ala-**Ala**-{Cys-Lys-Asn-Phe-Phe-Trp-Lys-Thr-Phe-Thr-Ser-Cys}-NH_2	9.7	9.8	9.1	<9.7	8.9
9	Ala^4-SRIF-14-NH_2: H-Ala-Gly-{Cys-**Ala**-Asn-Phe-Phe-Trp-Lys-Thr-Phe-Thr-Ser-Cys}-NH_2	9.1	9.3	8.6	<9.5	9.0
10	Ala^5-SRIF-14-NH_2: H-Ala-Gly-{Cys-Lys-**Ala**-Phe-Phe-Trp-Lys-Thr-Phe-Thr-Ser-Cys}-NH_2	9.6	9.9	9.2	<9.7	9.8
11	Ala^6-SRIF-14-NH_2: H-Ala-Gly-{Cys-Lys-Asn-**Ala**-Phe-Trp-Lys-Thr-Phe-Thr-Ser-Cys}-NH_2	6.9	7.7	6.7	<7.1	7.0
12	Ala^7-SRIF-14-NH_2: H-Ala-Gly-{Cys-Lys-Asn-Phe-**Ala**-Trp-Lys-Thr-Phe-Thr-Ser-Cys}-NH_2	7.7	7.7	7.6	<8.7	7.1
13	Ala^8-SRIF-14-NH_2: H-Ala-Gly-{Cys-Lys-Asn-Phe-Phe-**Ala**-Lys-Thr-Phe-Thr-Ser-Cys}-NH_2	6.0	6.0	6.0	<6.0	7.1
14	Ala^9-SRIF-14-NH_2: H-Ala-Gly-{Cys-Lys-Asn-Phe-Phe-Trp-**Ala**-Thr-Phe-Thr-Ser-Cys}-NH_2	6.0	6.0	6.0	<6.0	7.0
15	Ala^{10}-SRIF-14-NH_2: H-Ala-Gly-{Cys-Lys-Asn-Phe-Phe-Trp-Lys-**Ala**-Phe-Thr-Ser-Cys}-NH_2	8.2	9.0	8.8	<8.4	9.2
16	Ala^{11}-SRIF-14-NH_2: H-Ala-Gly-{Cys-Lys-Asn-Phe-Phe-Trp-Lys-Thr-**Ala**-Thr-Ser-Cys}-NH_2	9.2	8.2	8.1	<9.0	8.2
17	Ala^{12}-SRIF-14-NH_2: H-Ala-Gly-{Cys-Lys-Asn-Phe-Phe-Trp-Lys-Thr-Phe-**Ala**-Ser-Cys}-NH_2	9.3	8.9	9.2	<9.2	9.4
18	Ala^{13}-SRIF-14-NH_2: H-Ala-Gly-{Cys-Lys-Asn-Phe-Phe-Trp-Lys-Thr-Phe-Thr-**Ala**-Cys}-NH_2	9.8	10.1	9.2	<10.0	9.1
19	cyclo[HyPro-Phe-D-Trp-Lys-Tyr(Bzl)-Phe]	7.2	9.1	8.8	6.5	9.5
20	cyclo[(diaminopentylcarbamoyl)HyPro-Phe-D-Trp-Lys-Tyr(Bzl)-Phe]	8.0	8.5	8.7	6.2	9.2
21	cyclo[(diaminoethylcarbamoyl)HyPro-Phe-D-Trp-Lys-Tyr(Bzl)-Phe]	8.4	8.7	9.1	6.3	9.4
22	cyclo[(diaminoethylcarbamoyl)HyPro-His-D-Trp-Lys-Tyr(Bzl)-Phe]	8.4	9.1	9.1	<7.0	8.5
23	cyclo[(diaminoethylcarbamoyl)HyPro-Tyr-D-Trp-Lys-Tyr(Bzl)-Phe]	8.8	9.1	9.2	<7.0	9.6
24	cyclo[(diaminoethylcarbamoyl)HyPro-Arg-D-Trp-Lys-Tyr(Bzl)-Phe]	8.2	8.0	7.7	6.5	9.4
25	cyclo[(diaminoethylcarbamoyl)HyPro-Phg-D-Trp-Lys-Tyr(Bzl)-Phe], SOM230	8.2	9.0	9.1	<7.0	9.9
26	cyclo[(*N*,*N*-dimethyldiaminoethylcarbamoyl)HyPro-Phe-D-Trp-Lys-Tyr(Bzl)-Phe	8.8	9.3	9.5	<7.0	10.0

Scheme 1. Synthesis of Fmoc−(2*S*,4*R*)-(4-OCO−NH−CH_2−CH_2−NH−Boc)−Pro−OH (**32**)[a]

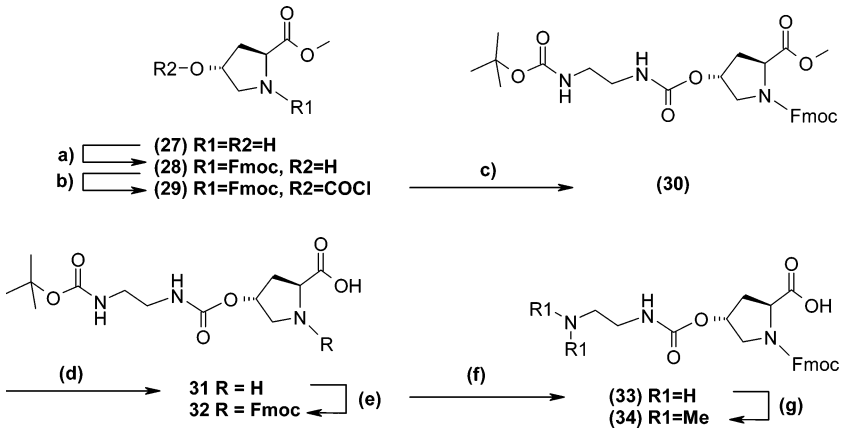

[a] (a) Fmoc-HOSu 1.1 equiv, 1 N $NaHCO_3$, THF, 18 h at room temp, 85%; (b) trisphosgene 0.6 equiv, THF, 3 h at room temp; (c) Boc-diaminoethane 5.0 equiv, (dimethylamino)pyridine 1.0 equiv, room temp, 49% over steps b and c; (d) 1 N NaOH, dioxane/H_2O; (e) Fmoc-HOSu 0.2 equiv, 1 N $NaHCO_3$, THF, 18 h at room temp, 71% over steps d and e; (f) TFA/H_2O, 95:5, 1 h at room temp, 95%; (g) formaldehyde (formalin) 10 equiv, H_2O/$NaCNBH_3$, 1 h at room temp, 89%.

were achieved by treatment with 95% TFA. Purification was carried out using RP-HPLC, and structural identity was confirmed by MS, NMR, and amino acid analysis. Strategies for synthesizing cyclohexapeptide SRIF mimics have included both solid-phase approaches and fragment condensation approaches in solution.[29,30] In this research, cyclohexapeptides **5**−**7** and **19**−**26** (Figure 1**)** were synthesized on solid phase using the Fmoc/^{t}Bu strategy and the SASRIN linker prior to cyclization in solution. Exemplified is the synthesis of SOM230 (**25**).

Synthesis of the required hydroxyproline amino acid derivatives was carried out in solution as illustrated in Scheme 1. Hydroxyproline methyl ester **27** was protected with Fmoc in a two-phase THF/1 N $NaHCO_3$ system overnight, providing **28**[31] in 85% yield. This fully protected Fmoc-hydroxyproline methyl ester was reacted with trisphosgene to provide the chlorocarbonate derivative **29**, which was then directly reacted with tertiary butyloxycarbonyl (Boc) diaminoethane in the presence of DMAP in THF, providing **30** in 49% yield. The methyl ester **30** was then cleaved to the free acid by treatment with 1 N NaOH in dioxane/water, providing a mixture of H−(2*S*,4*R*)-(4-OCO−NH−CH_2−CH_2−NH−Boc)−Pro−OH (**31**) and the desired product Fmoc−(2*S*,4*R*)-(4-OCO−NH−CH_2−CH_2−NH−Boc)−Pro−OH (**32**). Addition of 0.2 equiv of Fmoc-OSu resulted in reprotection of **31**, providing a further crop of **32** with a yield of 71%. For further derivatization, removal of the Boc side chain protecting group with 95% TFA/H_2O provided **33** in 95% yield, which readily underwent reductive amination with $NaCNBH_3$ and formaldehyde to provide **34** in 89% yield.

Synthesis of the linear peptide **35**, illustrated in Scheme 2, was achieved with slight modifications to a standard stepwise solid-phase procedure on a commercially available polystyrene resin containing the

Scheme 2. Solid-Phase Synthesis of SOM230

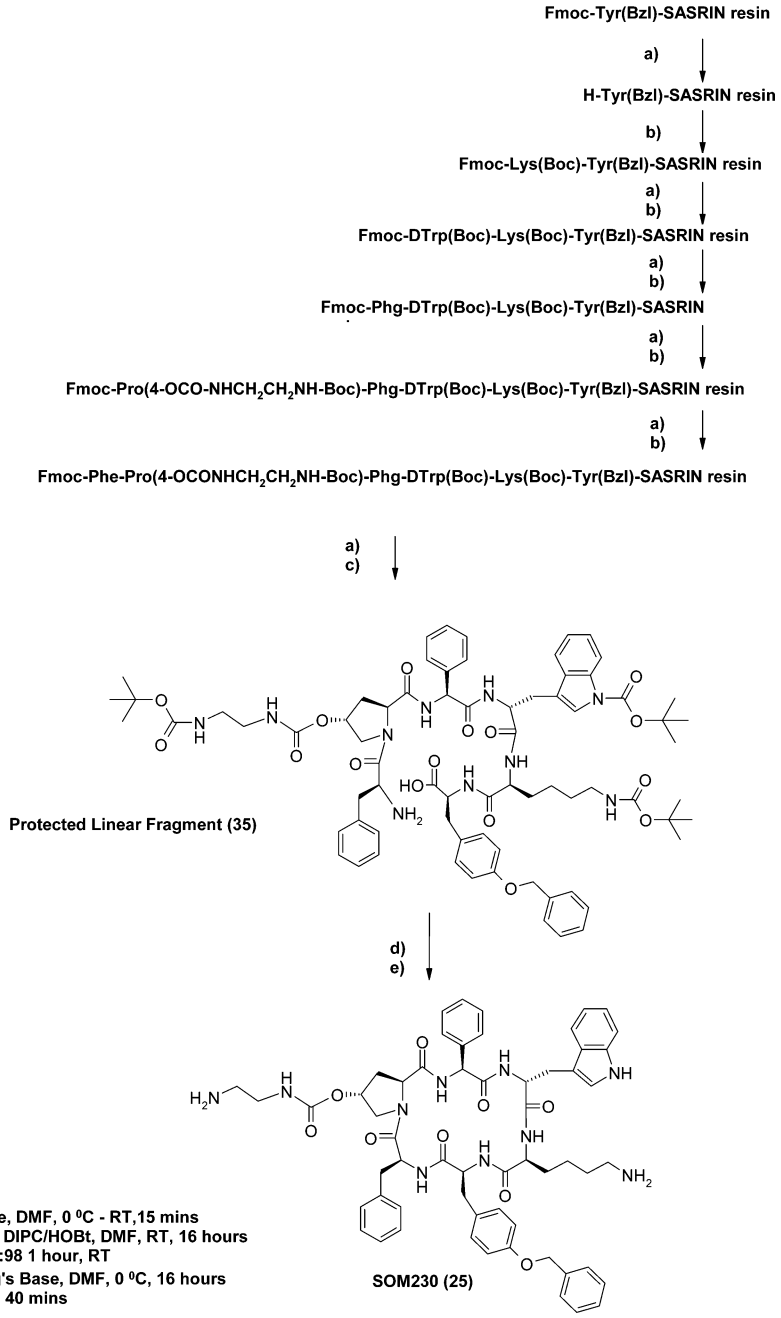

acid-cleaveable SASRIN linker. The base-labile fluorenylmethoxycarbonyl (Fmoc) group was used for Nα-amino protection, and side chains were protected by Boc protecting groups. Special care was taken to minimize racemization of phenylglycine by carrying out coupling of this amino acid at 0 °C. Furthermore, Fmoc deprotection steps after incorporation of phenylglycine were carried out at 0 °C utilizing less basic diethylamine instead of piperidine accompanied by very rapid washing. The assembled linear peptide was cleaved from its resin support by a short treatment with 2% TFA, leaving its side chain protection intact. Subsequently the side chain protected linear peptide was cyclized in DMF using diphenylphosphorylazide (DPPA). Finally side chain deprotection was achieved by treatment with 95% TFA. After purification by RP-HPLC, the desired product **25** was obtained in an overall yield of 20% and with 98% purity by HPLC. Its structural identity was confirmed by MS, NMR, and amino acid analysis.[32]

2.2. Pharmacology. SRIF Receptor Subtype Binding Studies. Results of SRIF receptor subtype binding studies are illustrated in Table 1 and Figures 2 and 3. Binding experiments were performed with membranes prepared from CHO (hsst1−hsst4) and COS (hsst5) cells expressing the respective human SRIF receptor subtype as reported previously.[33] $Tyr^{11}[^{125}I]$-SRIF was used as the SRIF receptor-specific radioligand. Radioligand binding was determined by incubating membranes for 1 h at room temperature in the presence or absence of various concentrations of unlabeled SRIF (**1**) or the respective analogue. The incubation was stopped by rapid filtration through Whatman GF/C glass fiber filters and subsequent washing. Specific binding was measured as the total $Tyr^{11}[^{125}I]$-SRIF binding minus

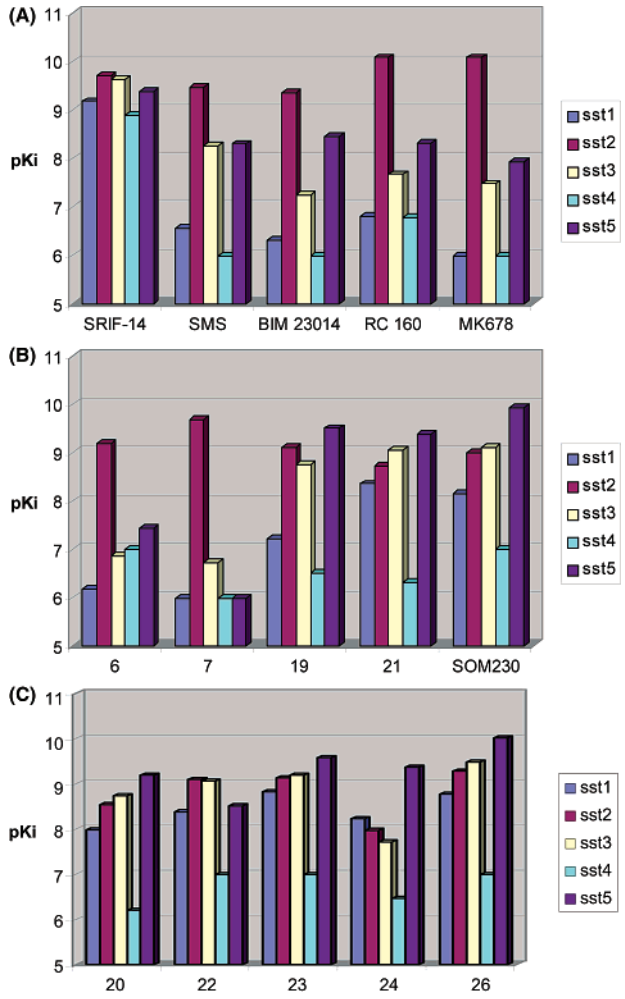

Figure 2. Drug design and structure−activity relationships.

the amount of radioligand bound in the presence of 100 nM SRIF-14 (**1**) (nonspecific binding).

3. Discussion

Drug Design and SAR Based on Receptor Binding Studies. In Figure 1, the structural features of SRIF-14 (**1**), **2**, **3**, **5**, and related analogues as well as **25** are illustrated. Essential structural features of **1** include the β-turn comprising amino acids, tryptophan (Trp), and lysine (Lys) as well as the cysteine−cysteine (Cys−Cys) bridge between position 3 and terminal position 14. The reduced size analogues can be subdivided into two structural classes: (I) cyclooctapeptides containing a Cys−Cys bridge (**2**, **3** and **4**) and (II) cyclohexapeptides where the ring structure is formed by a cyclic lactam (**5** and the newly discovered somatostatin analogue **25**). In both structural classes of reduced size analogues, the β-turn is stabilized by incorporation of the D-Trp.

It could be shown, in line with published data, that SRIF-14 exhibits high-affinity binding to each of the somatostatin receptor subtypes, in contrast to the cyclooctapeptides **2**−**4** and cyclohexapeptide **5** (Table 1, Figure 2A). Cyclooctapeptide **2** and cyclohexapeptide **5** show selective high-affinity binding to sst2 along with reduced binding to sst3 and sst5 but almost no binding to sst1 and sst4. On closer examination, cyclohexapeptide **5** seemed to have higher affinity to sst2 and lower affinity to sst3 and sst5 when compared to cyclooctapeptide **2**. In Figure 2B, the different cyclohexapeptides L-363,301 (**6**) and the hydoxyproline (HyPro) analogue of L-363,301 (**7**) are compared with respect to their binding to SRIF receptor subtypes. Both of these closely related cyclohexapeptide analogues exhibit high-affinity binding to sst2 but no binding to sst1. The NMe-Ala^1 containing **5** (Figure 2A) shows higher affinity to sst3 than the less flexible Pro^1 and HyPro^1 analogues. The Pro^1 analogue **6** shows higher affinity to sst4 than the other two cyclohexapeptides. Interestingly, the HyPro analogue **7** exhibits markedly less affinity to sst5 than the other two. These results provided a starting point for a rational approach to introducing new structural elements into a cyclohexapeptide template to enable high-affinity binding to the five SRIF receptor subtypes.

To approach this study rationally, it was considered that an "Ala-Scan" of SRIF-14 (**1**),[27] where amino acid residues are replaced with alanine in turn (except residues 3 and 14, forming the disulfide bridge, as well as residue 1, already an alanine), would enable comparison of the binding affinities of each alanine analogue for the five cloned SRIF receptor subtypes. Such a study would provide pivotal insights into the structural basis of the characteristic high-affinity binding of SRIF-14. Eleven "Ala-Scan" analogues, illustrated in Table 1 (**8**−**18**), were synthesized in the form of the Cys-terminal amides, Ala^n-SRIF-14-NH_2, which are more stable than Cys^{14}-OH analogues, using the Rink amide resin. As expected, the "Ala-Scan" (Figure 3) showed clearly that the β-turn region, consisting of Trp^8 and Lys^9, is essential for high-affinity binding to each of the cloned SRIF receptor subtypes sst1−sst5. Interestingly, it also became immediately apparent that the binding results of the "Ala-Scan" analogues can be divided into two distinct groups, sst1 and sst4 forming one closely related group, contrasting with sst2, sst3, and sst5, which form the second group. Indeed, this is exactly in parallel with the degree of sequence homology of the SRIF receptor subtypes previously reported.[8]

In addition to the anticipated result from the "Ala-Scan" that the β-turn region, consisting of Trp^8 and Lys^9, is essential for high-affinity binding to sst1−sst5, the role of the lipophilic Phe^6, Phe^7, and Phe^{11} of SRIF-14 emerged as being essential for high-affinity binding to sst2, sst3, and sst5. For sst1 and sst4, the pattern is different. While Phe^6 and Phe^7 were very important for high-affinity binding to sst1, only Phe^6 appeared to improve markedly sst4 binding, exemplified by **11**, **12**, and **16** illustrated in Table 1. In addition to the importance of Phe^6, Phe^7, and Phe^{11} for universal binding, another important hint emerged from the "Ala-Scan". Replacement of Lys^4 with Ala showed a reduction in high-affinity binding to sst2, sst3, and sst5, with Δ pK_i for sst2, sst3, and sst5 being −0.4, −1.0, −0.4 units, respectively. Once again, sst1 and sst4 were distinctly different with almost no effect on substitution of Lys^4 with Ala^4 on sst1 and even an increase in binding affinity being observed on substitution of Lys^4 with Ala^4 in the case of sst4.

In view of these results, it was considered that transposition of lipophilic functional groups mimicking Phe^6, Phe^7, and Phe^{11} of SRIF-14 (**1**) in addition to

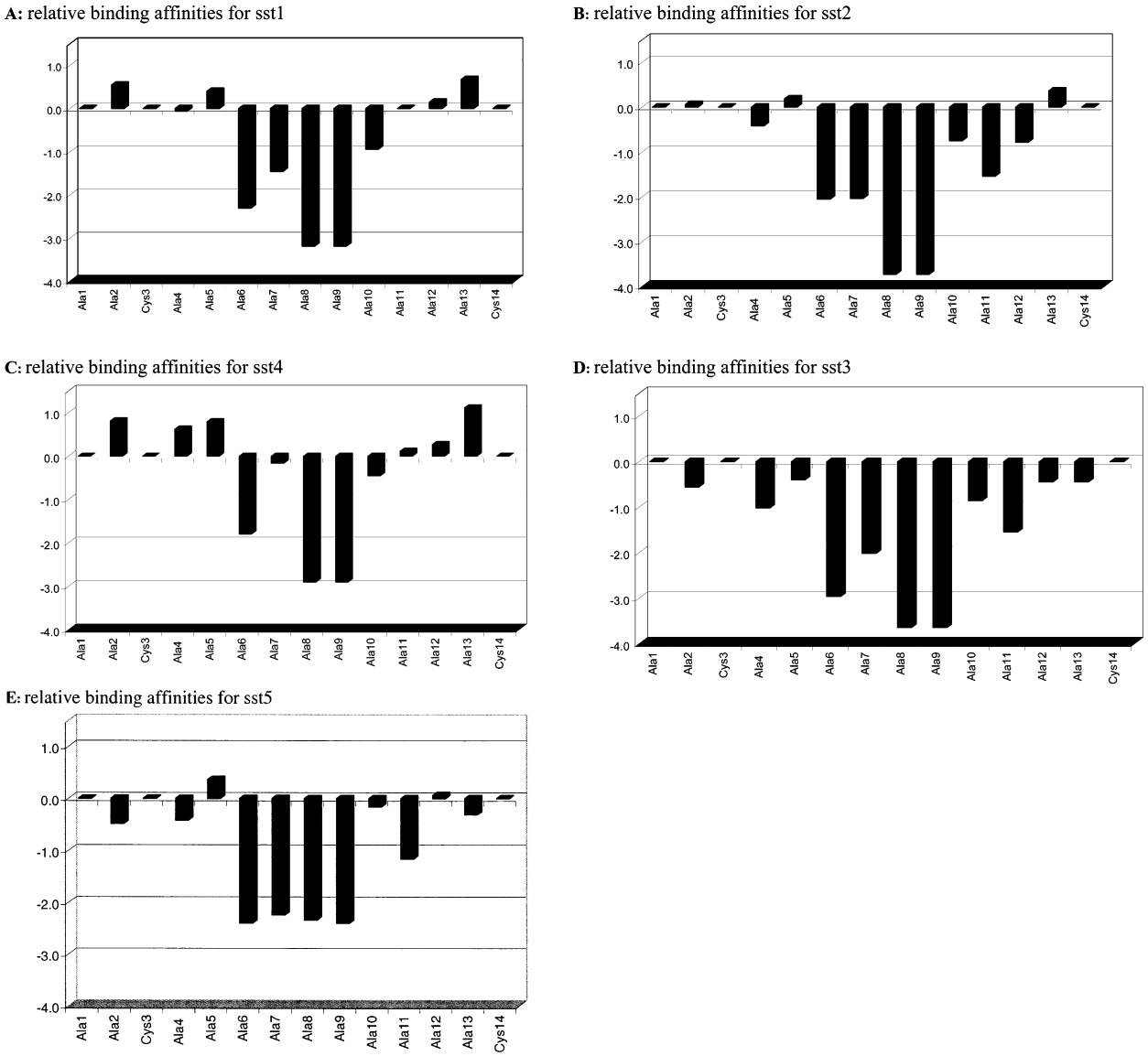

Figure 3. "Ala-Scan" of SRIF-14, comparing binding affinities of each analogue relative to SRIF-14 to the cloned SRIF receptor subtypes: (Y axis) δ pK_i (δ pK_i = p$K_{i(analogue)}$ − p$K_{i(SRIF)}$); (X axis) residue of SRIF-14 replaced by alanine. Residues 3 and 14, forming the disulfide bridge, were not replaced in the "Ala-Scan". Residue 1, already an alanine, was also not replaced.

transposition of a basic functional group mimicking Lys[4] of **1** into the reduced size, stable cyclohexapeptide template could lead to hitherto unattained high-affinity binding to a wider range of SRIF receptor subtypes.

In Figure 2B, this rational approach to reduced size, stable, universal somatostatin mimics is further illustrated. As starting points, the contrasting binding affinities of SRIF-14 (**1**), **2**, and **5** illustrated in Figure 2A and the differing but closely related binding affinities of the cyclohexapeptides **6** and its HyPro[1] analogue **7** illustrated in Figure 2B were considered. Achievement of "SRIF-14-like" universal high-affinity binding to SRIF receptor subtypes from a more rigid, reduced size cyclohexapeptide template was considered an extremely challenging goal. However, we considered that capitalizing on the detailed studies of receptor binding properties of the known cyclohexapeptides, combined with the pivotal results from the "Ala-Scan" (shown in Figure 3), would justify this SAR-based medicinal chemistry approach.

As the first step, the Phe[6], Phe[7], and Phe[11] of SRIF-14 (**1**) were mimicked by transposing these lipophilic functional groups into the cyclohexapeptide template in the form of a combination of Phe[2] and Tyr(Bzl)[5] substituting for Thr[5] (cyclohexapeptide numbering). The combination of the Phe[2] and Tyr(Bzl)[5] constituent amino acids incorporated within the reduced size cyclohexapeptide **19** provided for the first time an enhancement of binding to sst3 and sst5 along with continued high-affinity binding to sst2, as illustrated in Figure 2B.

Against expectation, this very encouraging result showing clearly that transposition of functional groups from SRIF-14 (**1**) into the cyclohexapeptide template could be accompanied by the associated receptor subtype binding characteristics prompted further exploration of this approach. As the second step, incorporation of a functionalized *trans*-hydroxyproline with a basic extension intended to mimic the Lys[4] of SRIF-14 was investigated, as illustrated in parts B and C of Figure 2. More precisely, diaminopentylcarbamoyl-Pro[1] and diaminoethylcarbamoyl-Pro[1] were incorporated into **20** and **21**, respectively, in combination with Tyr(Bzl)[5]. This resulted in unimpaired high-affinity binding to sst2, sst3, and sst5 accompanied for the first time by unexpected

high-affinity binding to sst1, with the shorter constituent diaminoethylcarbamoyl-Pro[1] in **21** being superior to the more extended diaminopentylcarbamoyl-Pro[1] extension incorporated in **20**. Indeed, from the "Ala-Scan", Lys[4] of SRIF-14 was implicated in high-affinity binding to sst2, sst3, and sst5. However, when incorporated into the reduced size, stable cyclohexapeptide template, the diaminoethylcarbamoyl-Pro[1] lysine mimic provided high-affinity binding to sst1. The final optimization of the cyclohexapeptide was achieved by adjusting the aromatic groups with the replacement of Phe[2] with phenylglycine[2] in combination with Tyr(Bzl)[5] and the diaminoethylcarbamoyl-Pro[1] basic extension, providing **25** exhibiting high-affinity binding to sst1, sst2, sst3, and sst5 as illustrated in Figure 2B.

The potential of this approach for optimization toward selectivity or alternatively toward high-affinity binding to several SRIF receptor subtypes is illustrated in Figure 2C. In the cases of **22** and **23**, incorporation of His[2] or Tyr[2] provides a ligand exhibiting high affinity to sst1, sst2, sst3, and sst5. In marked contrast, incorporation of Arg[2] in the case of **24** affords a cyclohexapeptide with more selective high-affinity binding to sst5 but strongly reduced affinities to sst1, sst2, sst3.[32] Variations in the length of the basic hydroxyproline urethane extension, such as **20**, which incorprates the diaminopentylcarbamoyl[1] extension combined with the remaining features of **21**, or bis-methylation of the basic hydroxyproline urethane extension **26**, which was however synthetically more cumbersome, additionally provides ligands exhibiting high affinities to sst1, sst2, sst3, and sst5.

4. Conclusion and Outlook

The strategy pursued in this research has been rewarded with the demonstrated superiority of **25** compared to **2**. Pharmacological studies in vitro[34] have clearly shown that **25** effectively inhibited the growth hormone releasing hormone (GHRH) induced growth hormone (GH) release in primary cultures of rat pituitary cells with an IC_{50} of 0.4 ± 0.1 nmol/L ($n = 5$). In vivo, **25** also potently suppressed GH secretion in rats.[34] The ED_{50} values determined at 1 and 6 h after injection of **25** indicated its very long duration of action in vivo. In the rat, **25** strongly decreases IGF-1 plasma levels, with the efficacy being markedly enhanced compared with the effects elicited by **2** after 7 days of treatment.[35] Furthermore, in rats, dogs, and rhesus monkeys, **25** potently and dose-dependently decreased IGF-1 levels for prolonged periods of time without desensitization as observed with SMS 201-995 (**2**).[35]

Whether selective sst ligands or alternatively universal ligands such as **25** will have a broader scope of therapeutic application is currently unknown. Predictions are difficult because one sst subtype such as sst2 is associated with more than one biological response so that selective binding would not translate into selectively triggering a certain response. Moreover, various sst subtypes can form heterodimers that differ in their affinity from the individual receptors; e.g., sst2A−sst3 heterodimers bind the universal ligand SRIF14 and a selective sst2 ligand but fail to bind a sst3-selective ligand. This is further complicated by the fact that receptor crosstalk leads to changes in receptor up- and down-regulation; e.g., a ligand selectively binding to sst5 induces up-regulation of sst1. Thus, a selective ligand for individual SRIF receptors also affects other sst subtypes. It is important to note that **25**, a nearly universal ligand, shows very favorable pharmacological effects regarding inhibition of the GH/IGF-1 axis so that the concept of mimicking the natural ligand SRIF-14 pharmacologically as closely as possible apparently translates into a promising therapeutic potential. Consequently, the superiority of **25** over **2**, derived from the unique broad receptor binding profile of **25**, should ultimately be compared to other approaches to somatostatin mimics.[36−44] Indeed, the pronounced inhibitory effects of **25** on the GH/IGF-1 axis has made this compound an ideal candidate drug for clinical studies in patients with acromegaly, especially in therapy-resistant cases where current therapies fail to adequately control elevated GH and IGF-1 levels.[24] Furthermore, potential future clinical applications may also include otherwise nontreatable somatostatin receptor-positive breast, prostate, and colonic cancers, as well as malignant lymphomas.[24] Since most endocrine tumors that are targets for somatostatin analogue therapy simultaneously express multiple but variable numbers of the different receptor subtypes, one would expect that a GH-secreting pituitary tumor that simultaneously expresses sst2 and sst5 would respond advantageously to **25** compared to **2)**.[24]

5. Experimental Section

5.1. Synthesis. 5.1.1. Synthesis of "Ala-Scan" Analogues. Commercially available Fmoc Rink amide functionalized resin, typically in the amount of 700 mg and with a loading of 0.47 mmol/g, was used as starting material in a manually operated reactor and carried through a standard protocol consisting of repetitive cycles of Nα deprotection (piperidine/DMF, 2:8), repeated washings with DMF, and coupling (DIPCI/HOBT, DMF). Couplings were continued or repeated until completion, i.e., until complete disappearance of residual amino groups when monitored with the "Kaiser" ninhydrin test. For cleavage and deprotection, the peptide resin was treated with TFA/H_2O, 95:5, for 30 min. Subsequently, Cys-S^{t}Bu protecting groups were removed with tributylphosphine, and oxidative cyclization was carried out in a dioxane/water solution with 2.5 ppm hydrogen peroxide to provide the crude product. The crude product was then precipitated with ether containing ca. 10 equiv of HCl, filtered, washed with ether, and dried. Purification was carried out using reversed-phase preparative HPLC. Yield was determined, accounting for the proportion of resin cleaved and the salt content, which is typically 5−20% depending on the cyclization.

H-Ala-Ala-{Cys-Lys-Asn-Phe-Phe-Trp-Lys-Thr-Phe-Thr-Ser-Cys}-NH_2 (8): 30 mg from 820 mg of resin, 99% purity, $Rt_I = 10.67$.

H-Ala-Gly-{Cys-Ala-Asn-Phe-Phe-Trp-Lys-Thr-Phe-Thr-Ser-Cys}-NH_2 (9): 25 mg from 700 mg of resin, 99% purity, $Rt_I = 13.74$.

H-Ala-Gly-{Cys-Lys-Ala-Phe-Phe-Trp-Lys-Thr-Phe-Thr-Ser-Cys}-NH_2 (10): 41 mg from 700 mg of resin, 98% purity, $Rt_I = 13.36$.

H-Ala-Gly-{Cys-Lys-Asn-Ala-Phe-Trp-Lys-Thr-Phe-Thr-Ser-Cys}-NH_2 (11): 65 mg from 700 mg of resin, 100% purity, $Rt_I = 10.16$.

H-Ala-Gly-{Cys-Lys-Asn-Phe-Ala-Trp-Lys-Thr-Phe-Thr-Ser-Cys}-NH_2 (12): 21 mg from 1000 mg of resin, 98% purity, $Rt_I = 11.34$.

H-Ala-Gly-{Cys-Lys-Asn-Phe-Phe-Ala-Lys-Thr-Phe-Thr-Ser-Cys}-NH_2 (13): 18 mg from 1000 mg of resin, 93% purity, $Rt_I = 9.27$.

H-Ala-Gly-{Cys-Lys-Asn-Phe-Phe-Trp-Ala-Thr-Phe-Thr-Ser-Cys}-NH_2 (14): 25 mg from 500 mg of resin, 96% purity, $Rt_I = 14.90$.

H-Ala-Gly-{Cys-Lys-Asn-Phe-Phe-Trp-Lys-Ala-Phe-Thr-Ser-Cys}-NH_2 (15): 14 mg from 500 mg of resin, 96% purity, $Rt_I = 12.68$.

H-Ala-Gly-{Cys-Lys-Asn-Phe-Phe-Trp-Lys-Thr-Ala-Thr-Ser-Cys}-NH_2 (16): 48 mg from 500 mg of resin, 99% purity, $Rt_I = 7.48$.

H-Ala-Gly-{Cys-Lys-Asn-Phe-Phe-Trp-Lys-Thr-Phe-Ala-Ser-Cys}-NH_2 (17): 61 mg from 1230 mg of resin, 98% purity, $Rt_I = 10.40$.

H-Ala-Gly-{Cys-Lys-Asn-Phe-Phe-Trp-Lys-Thr-Phe-Thr-Ala-Cys}-NH_2 (18): 80 mg from 1000 mg of resin, 100% purity, $Rt_I = 11.66$.

5.1.2. Synthesis of Amino Acids. 5.1.2.1. Synthesis of Fmoc−(2*S*,4*R*)-(4-OCO−NH−CH_2−CH_2−NH−Boc)−Pro−OH (32). As illustrated in Scheme 1, (2*S*,4*R*)-4-hydroxyproline methyl ester **27** (32.5 g, 224 mmol) was reacted with Fmoc-OSu in aqueous 1.0 N sodium carbonate/THF at room temperature. After completion of the reaction, Fmoc-(2S,4R)-4-hydroxyproline methyl ester **28** (70.0 g, 191 mmol) was isolated by precipitation in 85% yield. Fmoc-(2*S*,4*R*)-4-hydroxyproline methyl ester (70.0 g, 191 mmol) was then added dropwise into a solution of trisphosgene (33.8 g, 114 mmol, 0.6 equiv) in THF to give the Fmoc-(2*S*,4*R*)-4-chlorocarbonateproline methyl ester **29**. After 1 h, (dimethylamino)pyridine (23.4 g, 191 mmol, 1.0 equiv) and *N*-Boc-diaminoethane (152.8 g, 954 mmol, 5.0 equiv) were added and the reaction mixture was stirred at room temperature. After completion of the reaction, solvent was removed in vacuo and the Fmoc−(2*S*,4*R*)-(4-OCO−NH−CH_2−CH_2−NH−Boc)−Pro−OMe (**30**) was extracted from a two-phase system of ethyl acetate/0.1 M HCl to give the crude product ($MH^+ = 554$). Crystallization from ethyl acetate yielded Fmoc−(2*S*,4*R*)-(4-OCO−NH−CH_2−CH_2−NH−Boc)−Pro−OMe (**30**) (51.0 g, 92 mmol) in 95% purity and 49% yield. The methyl ester **30** (1.45 g, 2.6 mmol) was then cleaved to the free acid by treatment with 1 N NaOH in dioxane/water, providing a mixture of H−(2*S*,4*R*)-(4-OCO−NH−CH_2−CH_2−NH−Boc)−Pro−OH (**31**) and the desired product Fmoc−(2*S*,4R)-(4-OCO−NH−CH_2−CH_2−NH−Boc)−Pro−OH (**32**). Addition of 0.2 equiv of Fmoc-OSu resulted in reprotection of **31**, providing a further crop of **32** that underwent purification on silica gel: $(M + Na)^+ = 562$, 1.0 g, 1.85 mmol, yield 71%, purity 95%.

5.1.2.2. Synthesis of Fmoc−(2*S*,4*R*)-(4-OCO−NH−CH_2−CH_2−NMe_2)−Pro−OH (34). Fmoc−(2*S*,4*R*)-(4-OCO−NH−CH_2−CH_2−NH−Boc)−Pro−OH (**32**) (1.0 g, 1.85 mmol) was treated with TFA/H_2O, 95:5, and was preciptated into a solution of HCl in diethyl ether, providing Fmoc−(2*S*,4*R*)-(4-OCO−NH−CH_2−CH_2−NH_2)−Pro−OH (**33**) (0.80 g, 1.82 mmol) in 98% yield. Reductive amination was carried out using sodium cyanoborohydride and aqueous formaldehyde, providing **34** (0.76 g, 1.62 mmol), which was purified on slica gel: $(M + Na)^+ = 468$), yield 89%, purity 95%.

5.1.3. Solid-Phase Synthesis and Purification: Representative Procedure. Solid-phase synthesis was performed in a stirred batch reactor on a 7.2 mmol scale (two batches of 12.0 g of SASRIN resin, 0.6 mmol/g). An overall yield of 20% of purified **25** was obtained, relative to SASRIN resin. The effective peptide content for each batch was determined by amino acid analysis and varied between 70% and 73% ($F = 1.43$ and 1.37, respectively) for the two batches. Compound **25** as the trifluoroacetate salt is hygroscopic and should be stored cool and dry.

Preparative RP-HPLC was carried out on a C-18 10 μm STAGROMA column (5−25 cm) using a gradient of 0.5% TFA to 0.5% TFA in 70% acetonitrile. Fractions containing the pure compound were combined, diluted with water, and lyophilized. The synthesis was twice repeated in a stirred batch reactor on a 3 mmol scale and gave the product in a similar yield of 20% and a purity of >98% after purification. Ion exchange to the acetate salt was carried out with AGX3-X3 resin.

Analytical HPLC was typically carried out in the following systems.

For system I, buffer A was acetonitrile/water/phosphoric acid/tetramethylammonium hydroxide, 10:90:0.1:0.1 (v/v/v/v). Solvent B was acetonitrile/water/phosphoric acid/tetramethylammonium hydroxide, 140:60:0.8:2 (v/v/v/v). The gradient was 100% buffer A to 100% buffer B in 20 min.

For system II, buffer A was water/acetonitrile, 95:5, and 0.2% TFA. Buffer B was water/acetonitrile, 5:95, and 0.2% TFA. The gradient was 100% buffer A to 100% buffer B in 20 min.

For system III, buffer A was water and 0.1% TFA. Buffer B was acetonitrile and 0.1% TFA. The gradient was 20% buffer B to 100% buffer B in 30 min.

For system IV, as an alternative purification method, a semipreparative HPLC−MS system from Waters composed of a model 600 semipreparative pump, a model 7200 autosampler, a model 2487 UV detector, and an analytical model 515 dilution pump was used. A Symmetry C18 5 μm 50 mm × 19 mm column from Waters was used. The linear gradient was run in 9 min from 0% to 100% phase B with a flow of 20 mL/min. Phase A was water/acetonitrile, 95:5, with 0.1% trifluoracetic acid added. Phase B was water/acetonitrile, 5:95, with 0.1% trifluoracetic acid added. The MS signal was mesured with a LCZ platform from Waters. The operating conditions in ESI^+ mode were the following: source temperature, 120°C; desolvatation temperature, 400°C; ion energy, 1.0 V; capillary voltage 3.5 kV; cone voltage, 60 V; extractor, 3 V. The samples were dissolved in acetonitrile/water, 1:1, and an amount of 1000 μL of solution was injected.

5.1.3.1. Protected Linear Peptide Fragment H−Phe−(2*S*,4*R*)-(4-OCO−NH−CH_2−CH_2−NH−Boc)−Pro−Phg−D-Trp(Boc)−Lys(Boc)−Tyr(Bzl)−OH (35). Commercially available Fmoc−Tyr(Bzl)−O−CH_2−Ph(3-OCH_3)−O−CH_2−polystyrene resin (12.0 g, 7.2 mmol, 0.6 mmol/g SASRIN-resin) was used as starting material in a manually operated reactor and carried through a standard protocol consisting of repetitive cycles of Nα deprotection (piperidine/DMF, 2:8), repeated washings with DMF, and coupling (DIPCI/HOBT, DMF). The following amino acid derivatives were sequentially coupled: Fmoc−Lys(Boc)−OH, Fmoc−D-Trp(Boc)−OH, Fmoc−Phg−OH, Fmoc−(2*S*,4*R*)-(4-OCO−NH−CH_2−CH_2−NH−Boc)−Pro−OH, and Fmoc−Phe−OH. Couplings were continued or repeated until completion, i.e., until complete disappearance of residual amino groups when monitored with the "Kaiser" ninhydrin test.

Before cleavage of the completely assembled protected linear peptide from its resin support, Nα-Fmoc protection was removed. After washings with CH_2Cl_2, the peptide resin was transferred into a column and the peptide fragment was cleaved and eluted with a short treatment with 2% TFA in CH_2Cl_2. The eluate was immediately neutralized with a saturated $NaHCO_3$ solution. The organic solution was separated and evaporated. The side chain protected fragment was obtained in 93% homogeneity (HPLC), $MH^+ = 1366$, and cyclized without further purification.

5.1.3.2. Cyclization, Deprotection, and Purification of Cyclo[(diaminoethylcarbamoyl)-HyPro-Phg-D-Trp-Lys-Tyr(Bzl)-Phe] (25). For cyclization, the above linear fragment was dissolved in DMF to a concentration of 4 mM, cooled to −5 °C, treated with 2 equiv of DIPEA and then 1.5 equiv of DPPA, and stirred at 0−4 °C until completion (ca. 20 h). The solvent was almost completely removed in vacuo. The concentrate was diluted with ethyl acetate, washed with $NaHCO_3$ and water, dried, and evaporated in vacuo. The protected cyclized product was obtained in good yield.

For complete deprotection, the residue was dissolved at 0 °C in TFA/H_2O, 95:5 (ca. 50 mM), and the mixture was stirred in the cold for 30 min. The product was then precipitated with ether containing ca. 10 equiv of HCl, filtered, washed with ether, and dried. To completely decompose the remaining indole-N carbaminic acid, the product was dissolved in 5% AcOH and lyophilized after 15 h at ca. 5 °C. Analytical RP-HPLC indicated a purity of 75% for the crude product.

Table 2. ^{1}H and ^{13}C NMR Assignments of SOM230, Using Numbering Scheme in NMR Assignment

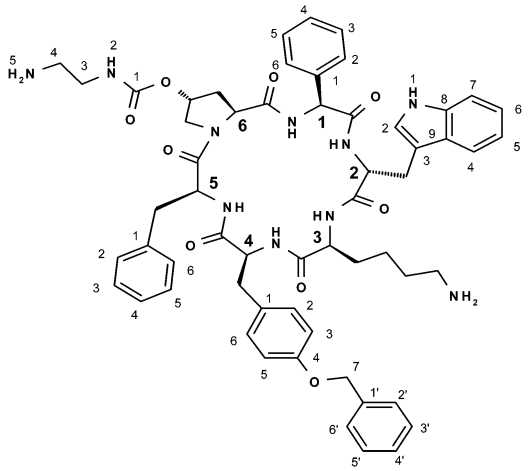

residue	group	δ ^{1}H [ppm]		δ ^{13}C [ppm]	residue	group	δ ^{1}H [ppm]		δ ^{13}C [ppm]
1	L-phenylglycine								
1	NH	9.73			1	α-CH	6.47		59.3
1	2/6-CH	8.02		127.3	1	CO			169.6
1	3/5-CH	7.41		129.1	1	1-C			141.0
1	4-CH	7.21		128.0					
2	D-tryptophane								
2	1′-NH	12.20			2	α-CH	5.28		55.6
2	NH	10.34			2	β-CH_2	3.72	3.30	28.5
2	7-CH	7.65		112.0	2	CO			173.9
2	4-CH	7.43		119.2	2	8-C			137.5
2	2-CH	7.28		124.7	2	9-C			128.3
2	6-CH	7.23		121.6	2	3-C			110.3
2	5-CH	6.96		119.2					
3	L-lysine								
3	NH	10.10			3	δ-CH_2	1.41	1.32	31.5
3	α-CH	4.62		55.2	3	γ-CH_2	0.89		23.5
3	ϵ-CH_2	2.80		41.0	3	CO			171.9
3	β-CH_2	1.87	1.32	31.6	3	NH_3^+	*a*		
4	(4-*O*-benzyl)-L-tyrosine								
4	NH	7.99			4	7-CH_2	4.92		69.9
4	2′/6′-CH	7.46		128.0	4	β-CH_2	3.46	3.10	39.7
4	3′/5′-CH	7.37		128.9	4	CO			171.8
4	4′-CH	7.30		128.2	4	4-C			157.9
4	2/6-CH	7.21		131.5	4	1′C			137.9
4	3/5-CH	6.85		114.7	4	1-C			129.8
4	α-CH	5.23		53.1					
5	L-phenylalanine								
5	NH	9.82			5	α-CH	4.42		53.9
5	2/6-CH	7.38		130.0	5	β-CH_2	3.23	3.06	37.8
5	3/5-CH	7.27		129.3	5	CO			171.2
5	4-CH	7.16		127.6	5	1-C			136.3
6	(γ-*O*-diaminoethylcarbamate)-l-hydroxyproline								
6	2-NH	8.04			6	4-CH_2	2.95		42.4
6	γ-CH	5.23		70.9	6	β-CH_2	2.63	1.25	37.0
6	α-CH	4.22		60.6	6	CO			170.7
6	δ-CH_2	4.12		51.4	6	1-CO			156.7
6	3-CH_2	3.42		44.5	6	4-NH_3^+	*a*		
A	acetate								
A	CH_3	2.20		22.1	A	CO			174.3

[a] The NH_3^+ protons are part of the water peak at 5.82 ppm.

Preparative HPLC purification afforded **25**: 3.1 g, 20% yield, purity 98%, Rt_I = 10.70, Rt_{II} = 10.20, Rt_{IV} = 3.90, HRMS 1047.51 (calcd 1047.5014).

Compounds **19**−**26** were synthesized using commercially available SASRIN resin, typically in the amount of 300 mg and with a loading of 0.65 mmol/g. Yield was determined, accounting for the proportion of resin cleaved and the salt content, which was typically 5−20% depending on the cyclization.

Cyclo[HyPro-Phe-D-Trp-Lys-Tyr(Bzl)-Phe] (19): 2.2 mg from 300 mg of resin, 94% purity, Rt_I = 11.11, Rt_{II} = 12.24. HRMS 975.4767 (calcd 975.4769).

Cyclo[(diaminopentylcarbamoyl)HyPro-Phe-D-Trp-Lys-Tyr(Bzl)-Phe] (20): 24 mg from 300 mg of resin, 96% purity, Rt_I = 4.58, Rt_{II} = 11.72, HRMS 1103.5716 (calcd 1103.5718).

Cyclo[(diaminoethylcarbamoyl)HyPro-Phe-D-Trp-Lys-Tyr(Bzl)-Phe] (21): 64 mg from 300 mg of resin, 96% purity, Rt_I = 3.16, Rt_{II} = 11.36, HRMS 1061.5247 (calcd 1061.5249).

Cyclo[(diaminoethylcarbamoyl)HyPro-His-D-Trp-Lys-Tyr(Bzl)-Phe] (22): 8.5 mg from 300 mg of resin, 100% purity, Rt_I = 10.12, Rt_{II} = 09.56, HRMS 1051.5152 (calcd 1051.5154).

Cyclo[(diaminoethylcarbamoyl)HyPro-Tyr-D-Trp-Lys-Tyr(Bzl)-Phe] (23): 7.2 mg from 300 mg of resin, 92% purity, Rt_I = 12.26, Rt_{II} = 10.62, HRMS 1077.5201 (calcd 1077.5198).

Cyclo[(diaminoethylcarbamoyl)HyPro-Arg-D-Trp-Lys-Tyr(Bzl)-Phe] (24): 3.3 mg from 300 mg of resin, 92% purity, Rt_I = 3.78, Rt_{III} = 9.44, HRMS 1070.5590 (calcd 1070.5576).

Cyclo[(diaminoethylcarbamoyl)HyPro-Phg-D-Trp-Lys-Tyr(Bzl)-Phe] (25): 3.1 g from 12 g of resin, 98% purity, Rt_I = 10.70, Rt_{II} = 10.20, Rt_{IV} = 3.90, HRMS 1047.51 (calcd 1047.5014).

Cyclo[(*N*,*N*-dimethyldiaminoethylcarbamoyl)HyPro-Phe-D-Trp-Lys-Tyr(Bzl)-Phe (26): 53 mg from 300 mg of resin, 97% purity, Rt_I = 14.53, Rt_{II} = 11.51, HRMS 1089.5561 (calcd 1089.5562).

5.1.4. Assignment of Amino Acid Configuration Using Amino Acid Analysis. A sensitive and selective method for the unambiguous assignment of the absolute configuration of the amino acids in **25** was utilized. Compound **25** was hydrolyzed under acidic conditions, and the individual amino acids were converted to the respective *N*(*O*)-trifluoroacetyl isopropyl esters. The separation of the enantiomers and assignment of the configuration of each amino acid were carried out by enantioselective gas chromatography/chemical ionization mass spectrometry. The expected configurations of the amino acids were proven.

5.1.5. NMR Assignment and Analysis. NMR spectra were measured at 300 K (27 °C) on a Bruker DMX 500 spectrometer using a selective probe for the 1D ^{13}C spectrum and a triple inverse probe for 1D ^{1}H and 2D spectra. Sample concentration was 10 mg in 0.5 mL of pyridine-d_5. ^{1}H and ^{13}C shifts are referenced to TMS (0 ppm). The following NMR experiments were carried out: (A) ^{1}H NMR, (B) ^{13}C NMR, (C) $^{1}H-^{1}H$ COSY, (D) $^{1}H-^{1}H$ ROESY, (E) $^{1}H-^{1}H$ TOCSY, (F) $^{1}H-^{13}C$ COSY, and (G) long-range $^{1}H-^{13}C$ COSY. The complete assignment of the NMR spectra is summarized in Table 2.

5.2. Pharmacological Characterization. Radioligand Binding Assays. Radioligand binding assays were performed as described previously.[33] Briefly, membranes from CHO and COS cells expressing the respective human SRIF receptor subtype were incubated with the SRIF receptor ligand Tyr^{11}-[^{125}I]-SRIF in the presence or absence of various concentrations of SRIF receptor ligands. The incubation was stopped after 1 h by rapid filtration through Whatman GF/C filters. Inhibition curves were analyzed, and IC_{50} values were calculated.[34]

Acknowledgment. R. Aichholz, K. Akyel, S. Arnold, G. Bovermann, E. Francotte, H. U. Gremlich, F. Kessler, J. M. Meisbuerger, L. Oberer, F. Roll, and C. Simeon are acknowledged for the syntheses and NMR, MS, HPLC, IR, UV, and amino acid analyses. Dr. Rudolf Duthaler, Novartis Leading Scientist, is acknowledged for excellent advice concerning this manuscript. Professor S. W. J. Lamberts, Rotterdam, is acknowledged for clinical perspectives.

Appendix

Abbreviations and Synonyms. SRIF, somatotropin release inhibitory factor; SMS 201-995, octreotide or Sandostatin; BIM 23014, lanreotide, Somatuline; RC160, vapreotide; MK-678, seglitide; Fmoc, fluorenylmethoxycarbonyl; Boc, *tert*-butyloxycarbonyl; HPLC, high-performance liquid chromatography; DIPC, diisopropylcarbodiimide; HOBt, hydroxybenzotriazole; DMF, dimethylformamide; CHO cells, Chinese hamster ovary cells; COS cells, SV40 transformed African green monkey kidney cells; GH, growth hormone; IGF-1, insulin-like growth factor-1; $pK_i = -\log(K_i)$; $K_i = IC_{50}/(1 + (L/K_d))$; $\delta\, pK_i = pK_{i(analogue)} - pK_{i(SRIF)}$; Rt_A, retention time utilizing system A.

Supporting Information Available: HRMS, NMR, IR, and GC spectra. This material is available free of charge via the Internet at http://pubs.acs.org.

References

(1) Brazeau, P.; Vale, W.; Burgus, R.; Ling, N.; Butcher, M.; Rivier, J.; Guillemin, R. Hypothalamic polypeptide that inhibits the secretion of immunoreactive pituitary growth hormone. *Science* **1973**, *179*, 77−79.

(2) Epelbaum, J. Somatostatin in the central nervous system: physiology and pathological modifications. *Prog. Neurobiol.* **1986**, *27*, 63−100.

(3) Hoyer, D.; Luebbert, H.; Bruns, C. Molecular pharmacology of somatostatin receptors. *Naunyn-Schmiedeberg's Arch. Pharmacol.* **1994**, *350* (5), 441−453.

(4) Bruns, C.; Weckbecker, G.; Raulf, F.; Kaupmann, K.; Schoeffter, P.; Hoyer, D.; Lubbert, H. Molecular pharmacology of somatostatin-receptor subtypes. *Ann. N. Y. Acad. Sci.* **1994**, *733* 138−46.

(5) Patel, Y. C. Somatostatin and its receptor family. *Front. Neuroendocrinol.* **1999**, *20*, 157−198.

(6) Hannon, J. P.; Bruns, C.; Weckbecker, G.; Hoyer, D. Somatostatin receptor gene family-subtype selectivity for ligand binding. In *Somatostatin*; Patel, Y. C., Ed.; in press.

(7) Reisine, T.; Bell, G. I. Molecular properties of somatostatin receptors. *Neuroscience* **1995,** *67*, 777−790.

(8) Reisine, T.; Bell, G. I. Molecular biology of somatostatin receptors. *Endocr. Rev.* **1995**, *16*, 427−442.

(9) Bruns, C.; Weckbecker, G.; Raulf, F.; Lübbert, H.; Hoyer, D. Characterization of somatostatin receptor subtypes. In *Somatostatin and Its Receptors*, Reichlin, S., Ed.; Ciba Foundation Symposium 190; Wiley: Chichester, 1995, pp 89−110.

(10) Froidevaux, S.; Eberle, A N. Somatostatin analogs and radiopeptides in cancer therapy. *Biopolymers* **2002**, *66* (3), 161−183.

(11) Bauer, W.; Briner, U.; Doepfner, W.; Haller, R.; Huguenin, R.; Marbach, P.; Petcher, T.; Pless, J. SMS 201-995: A very potent and selective analogue of Somatostatin with prolonged action. *Life Sci.* **1980**, *31*, 1134−1140.

(12) Murphy, W. A.; Lance, V A.; Moreau, S.; Moreau, J.; Coy, D H. Inhibition of rat prostate tumor growth by an octapeptide analog of somatostatin. *Life Sci.* **1987**, *40*, 2515−2522.

(13) Coy, D. H.; Taylor, J. E. Receptor-specific somatostatin analogues: Correlations with biological activity. *Metabolism* **1996**, *34* (1), 21−23.

(14) Cai, R. Z.; Szoke, B.; Lu, R.; Fu, D.; Redding, T. W.; Schally, A. V. Synthesis and biological activity of highly potent octapeptide analogs of somatostatin. *Proc. Natl. Acad. Sci. U.S.A.* **1986**, *83* (6), 1896−1900.

(15) Karashima, T.; Cai, R. Z.; Schally, A. V. Effects of highly potent octapeptide analogs of somatostatin on growth hormone, insulin and glucagon release. *Life Sci.* **1987**, *41*, 1011−1019.

(16) Patel, Y. C.; Wheatley, T. In vivo and in vitro plasma disappearance and metabolism of somatostatin-28 and somatostatin-14 in the rat. *Endocrinology* **1983**, *112* (1), 220−225.

(17) Lamberts, S. W. J.; Van Der Lely, A. J.; De Herder, W. W.; Hofland, L. J. Octreotide. *N. Engl. J. Med.* **1996**, *334*, 246−254.

(18) Veber, D. F.; Freidinger, R. M.; Perlow, D. S., Jr.; Palaveda, W. J.; Holly, F. W.; Strachan, R. G.; Nutt, R. F.; Arison, B. J.; Homnick, C.; Randall, W. C.; Glitzer, M. S.; Saperstein, R.; Hirschmann, R. A potent cyclic hexapeptide analogue of somatostatin. *Nature* **1981**, *292*, 55−58.

(19) Veber, D. F. Design of a highly active cyclic hexapeptide analogue of somatostatin. In *Peptides: Synthesis, Structure and Function. Proceedings of the Seventh American Peptide Symposium*; Rich, D. H., Gross, V. J., Eds.; Pierce Chemical Co.: Rockford, IL, 1981; pp 685−694.

(20) Veber, D. F.; Saperstein, R.; Nutt, R. F.; Freidinger, R. M.; Brady, S. F.; Curley, P.; Perlow, D. S.; Paleveda, W. J.; Colton, C. D.; Zacchei, A. G. A super active cyclic hexapeptide analog of somatostatin. *Life Sci.* **1984**, *34* (14), 1371−1378.

(21) Freidinger, R. M.; Perlow, D. S.; Randall, W. C.; Saperstein, R.; Arison, B. H.; Veber, D. F. Conformational modifications of cyclic hexapeptide somatostatin analogs. *Int. J. Pept. Protein Res.* **1984,** *23* (2), 142−150.

(22) Nutt, R. F.; Colton, C. D.; Saperstein, R.; Veber, D. F. Side Chain Conformations of Somatostatin Analogs When Bound to Receptors. In *Somatostatin*; Reichlin, S., Ed.; Plenum Publishing Corp.: New York, 1987; pp 83−87.

(23) Veber, D. F. Design and discovery in the development of peptide analogs. In *Peptides: Chemistry and Biology. Proceedings of the Twelfth American Peptide Symposium*; Smith, J. A., Rivier, J. E., Eds.; ESCOM, Leiden, 1992; pp 3−14.

(24) Lamberts, S. W. J.; van der Lely, A. J.; Hofland, L. J. New somatostatin analogs: Will they fulfil old promises? *Eur. J. Endocrinol.* **2002**, *146* (5), 701−705.

(25) Rohrer, S. P.; Birzin, E. T.; Mosley, R. T.; Berk, S. C.; Hutchins, S. M.; Shen, D. M.; Xiong, Y.; Hayes, E. C.; Parmar, R. M.; Foor, F.; Mitra, S. W.; Degrado, S. J.; Shu, M.; Klopp, J. M.; Cai, S. J.; Blake, A.; Chan, W. W.; Pasternak, A.; Yang, L.; Patchett, A. A; Smith, R. G; Chapman, K. T.; Schaeffer, J. M. Rapid identification of subtype-selective agonists of the somatostatin receptor through combinatorial chemistry. *Science (Washington, D.C.)* **1998**, *282*, 737−740.

(26) Yang, L.; Berk, S. C.; Rohrer, S. P.; Mosley, R. T.; Guo, L.; Underwood, D. J.; Arison, B. H.; Birzin, E. T.; Hayes, E. C.; Mitra, S. W.; Parmar, R. M.; Cheng, K.; Wu, T. J.; Butler, B. S.; Foor, F.; Pasternak, A.; Pan, Y.; Silva, M.; Freidinger, R. M.; Smith, R. G.; Chapman, K.; Schaeffer, J. M.; Patchett, A A. Synthesis and biological activities of potent peptidomimetics selective for somatostatin receptor subtype 2. *Proc. Natl. Acad. Sci. U.S.A.* **1998**, *95*, 10836−10841.

(27) Rivier, J.; Brown, M.; Rivier, C.; Ling, N.; Vale, W. Hypothalamic hypophysiotropic hormones: review on the design of synthetic analogs. In *Peptides 1976*; Loffet, A., Eds.; Editions de l'Universites: Bruxelles, Belgium, 1976; Vol. V; pp 427−521.

(28) Bernatowicz, M. S.; Daniels, S. B.; Koster, H. A comparison of acid-labile linkage agents for the synthesis of peptide C-terminal amides. *Tetrahedron Lett.* **1989,** *30* (35), 4645−4648.

(29) Mattern R.-H.; Moore, S. B.; Tran, T.-A.; Rueter, J. K.; Goodman, M. Synthesis, Biological Activities and Conformational Studies of Somatostatin Analogs. *Tetrahedron* **2000**, *56*, 9819−9831.

(30) Falb, E.; Salitra, Y.; Yechezkel, T.; Bracha, M.; Litman, P.; Olender, R.; Rosenfeld, R.; Senderowitz, H.; Jiang, S.; Goodman, M. A bicyclic and hsst2 selective somatostatin analogue: design, synthesis, conformational analysis and binding. *Bioorg. Med. Chem.* **2001**, *9* (12), 3255−3264.

(31) Thompson, L. A.; Ellman, J. A. Straightforward and general method for coupling alcohols to solid supports. *Tetrahedron Lett.* **1994**, *35* (50), 9333−9336.

(32) Lewis, I.; Bauer, W.; Albert, R.; Chandramouli, N.; Pless, J.; Engel, G.; Weckbecker, G.; Bruns, C. Rational approach to stable, universal somatostatin analogues with superior therapeutic potential. In *Peptides: The Wave of the Future. Proceedings of the Second International and the Seventeenth American Peptide Symposium*; Houghten, R., Lebl, M., Eds.; American Peptide Society: San Diego, CA, 2001; pp 718−720.

(33) Bruns, C.; Raulf, F.; Hoyer, D.; Schloos, J.; Luebbert, H.; Weckbecker, G.; Binding properties of somatostatin receptor subtypes. *Metab., Clin Exp.* **1996**, *44* (8, Suppl. 1), 17−20.

(34) Bruns, C.; Lewis, I.; Briner, U.; Meno-Tetang, G.; Weckbecker, G. SOM230: a novel somatostatin peptidomimetic with a broad somatotropin release inhibiting factor (SRIF) receptor binding and a unique antisecretory profile. *Eur. J. Endocrinol.* **2002**, *146*, 707−716.

(35) Weckbecker, G.; Briner, U.; Lewis, I.; Bruns, C. SOM230: a new somatostatin peptidomimetic with potent inhibitory effects on the growth hormone/insulin-like growth factor-I axis in rats, primates, and dogs. *Endocrinology* **2002**, *143* (10), 4123−4130.

(36) Souers, A. J.; Virgilio, A. A.; Rosenquist, S. A.; Fenuik, W.; Ellman, J. A. Identification of a Potent Heterocyclic Ligand to Somatostatin Receptor Subtype 5 by the Synthesis and Screening of β-Turn Mimetic Libraries. *J. Am. Chem. Soc.* **1999**, *121* (9), 1817−1825.

(37) Gademann, K.; Kimmerlin, T.; Hoyer, D.; Seebach, D. Peptide folding induces high and selective affinity of a linear and small β-peptide to the human somatostatin receptor 4. *J. Med. Chem.* **2001**, *44* (15), 2460−2468.

(38) Rivier, J. E.; Hoeger, C.; Erchegyi, J.; Gulyas, J.; DeBoard, R.; Craig, A. G.; Koerber, S. C.; Wenger, S.; Waser, B.; Schaer, J.-C.; Reubi, J. C. Potent Somatostatin Undecapeptide Agonists Selective for Somatostatin Receptor 1 (sst1). *J. Med. Chem.* **2001**, *44* (13), 2238−2246.

(39) Rajeswaran, W. G.; Hocart, S. J.; Murphy, W. A.; Taylor, J. E.; Coy, D. H. Highly Potent and Subtype Selective Ligands Derived by *N*-Methyl Scan of a Somatostatin Antagonist. *J. Med. Chem.* **2001**, *44* (8), 1305−1311.

(40) Rajeswaran, W. G.; Hocart, S. J.; Murphy, W. A.; Taylor, J. E.; Coy, D. H. *N*-Methyl Scan of Somatostatin Octapeptide Agonists Produces Interesting Effects on Receptor Subtype Specificity. *J. Med. Chem.* **2001**, *44* (9), 1416−1421.

(41) Poitout, L.; Roubert, P.; Contour-Galcera, M.-O.; Moinet, C.; Lannoy, J.; Pommier, J.; Plas, P.; Bigg, D.; Thurieau, C. Identification of Potent Non-Peptide Somatostatin Antagonists with sst3 Selectivity. *J. Med. Chem.* **2001**, *44* (18), 2990−3000.

(42) Contour-Galcera, M.-O.; Poitout, L.; Moinet, C.; Morgan, B.; Gordon, T.; Thurieau, C. Synthesis of substituted imidazopyrazines as ligands for the human somatostatin receptor subtype 5. *Bioorg. Med. Chem. Lett.* **2001**, *11* (5), 741−745.

(43) Gazal, S.; Gelerman, G.; Ziv, O.; Karpov, O.; Litman, P.; Bracha, M.; Afargan, M.; Gilon, C. Human Somatostatin Receptor Specificity of Backbone-Cyclic Analogues Containing Novel Sulfur Building Units. *J. Med. Chem.* **2002**, *45* (8), 1665−1671.

(44) Reubi, J. C.; Eisenwiener, K.-P.; Rink, H.; Waser, B.; Macke, H. R. A new peptidic somatostatin agonist with high affinity to all five somatostatin receptors. *Eur. J. Pharmacol.* **2002**, *456* (1−3), 45−49.

JM021093T